

See discussions, stats, and author profiles for this publication at: <https://www.researchgate.net/publication/275772073>

# Syntheses, Structures, Luminescence, and Photocatalytic Properties of a Series of Uranyl Coordination Polymers

ARTICLE in CRYSTAL GROWTH & DESIGN · OCTOBER 2014

Impact Factor: 4.89 · DOI: 10.1021/cg501118b

---

CITATIONS

8

---

READS

14

5 AUTHORS, INCLUDING:



Weiting Yang

44 PUBLICATIONS 697 CITATIONS

SEE PROFILE



Lei Wang

Chinese Academy of Sciences

13 PUBLICATIONS 69 CITATIONS

SEE PROFILE



Zhong-Ming Sun

Changchun Institute of Applied Chemistry

85 PUBLICATIONS 1,676 CITATIONS

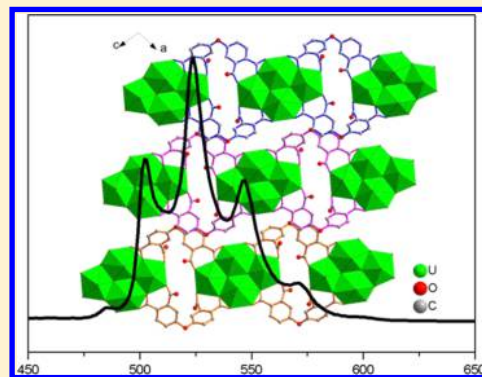
SEE PROFILE

## Syntheses, Structures, Luminescence, and Photocatalytic Properties of a Series of Uranyl Coordination Polymers

Weiting Yang,<sup>†</sup> Wan-Guo Tian,<sup>†,‡</sup> Xiao-Xiao Liu,<sup>†,‡</sup> Lei Wang,<sup>†</sup> and Zhong-Ming Sun<sup>\*,†</sup><sup>†</sup>State Key Laboratory of Rare Earth Resource Utilization, Changchun Institute of Applied Chemistry, Chinese Academy of Sciences, 5625 Renmin Street, Changchun, Jilin 130022, P. R. China<sup>‡</sup>School of Chemistry and Environmental Engineering, Changchun University of Science & Technology, Changchun 130022, China

## S Supporting Information

**ABSTRACT:** A new series of uranium coordination polymers have been hydrothermally synthesized by using 4,4'-oxidiphthalic acid ( $H_4L$ ) in the presence of N-bearing species, namely,  $(H_2dpa)UO_2L \cdot 3H_2O$  (**1**),  $(H_2dib)UO_2L \cdot H_2O$  (**2**),  $(H_2bbi)(UO_2)L \cdot 3H_2O$  (**3**),  $(H_2dib)(dib)_{0.5}[UO_2L(dib)] \cdot 3H_2O$  (**4**),  $(H_2bbi)(U_2O_5)L \cdot 2H_2O$  (**5**), and  $(Hbpi)_2(UO_2F_2)L$  (**6**) [ $dpa$  = di(pyridin-4-yl)amine,  $dib$  = 1,4-di(1H-imidazol-1-yl)benzene,  $bbi$  = 1,1'-(1,4-butanediyl)bis(imidazole), and  $bpi$  = 1-(biphenyl-4-yl)-1H-imidazole]. Compounds **1**–**3** exhibit the ribbon structures with  $dpa$ ,  $dib$ , and  $bbi$  as the templates, respectively. Compound **4** represents a one-dimensional chain assembly of uranyl centers,  $L$  ligands, and coordinated  $dib$  molecules. Compound **5** contains the tetranuclear motifs of edge-sharing of two  $UO_7$  pentagonal and two  $UO_8$  hexagonal bipyramids, which are linked by  $L$  ligands forming a layered structure with  $bbi$  as the template. Compound **6** forms a two-dimensional arrangement, in which the chain structures of edge-sharing  $UO_5F_2$  pentagonal bipyramids are pillared by  $L$  ligands. Luminescence studies reveal the characterized green light emission from uranyl centers for these uranyl carboxylates. Moreover, the excellent visible light photodegradation activities for RhB are displayed by these coordination polymers.



## ■ INTRODUCTION

In recent years, the rapid growth of the field of coordination polymers has received a great deal of attention because of their intriguing architectures and valuable properties.<sup>1</sup> The prospective structures and the unique properties are based on the selection of metal centers and organic ligands. Compared with commonly used rigid carboxylate ligands, flexible multicarboxylate ligands exhibit special advantages in their varied configurations from the flexible molecular backbones and versatile coordination modes, which thus lead to a wide variety of coordination polymers with attractive structures.<sup>2</sup> On the other hand, the inorganic metal centers also have pivotal effects on the final structures and the properties. In contrast to extensively employed transition metals and rare earth metals, actinides have been investigated less frequently via crystal engineering.<sup>3–5</sup> Indeed, coordination polymers of uranium, the representative of the actinide series, are of special research interest not only because of their fascinating structural diversity but also because of their promising photochemical properties, including photoluminescence, photocatalysis, photocurrent, and photovoltaic responses.<sup>6–10</sup> Hexavalent uranium is the most common state in nature, and a particular structural motif, uranyl  $UO_2^{2+}$  dication, is the usual form in  $U(VI)$  complexes. The coordination environment of the  $U(VI)$  center is flexible with six to eight atoms being capable of being coordinated. Thus, varied coordination fashions ranging from tetragonal and

pentagonal to hexagonal bipyramids are created, which can further polymerize, thereby forming a variety of polynuclear uranyl species. These bipyramidal polyhedra together with their various oligomers combining with the flexible multicarboxylate ligands mentioned above allow uranyl coordination polymers with appealing structures and interesting properties to be generated. For example, Cahill and Thuéry used flexible aliphatic carboxylic acids for the preparation of uranyl carboxylates with the structures varying from zero-dimensional to three-dimensional architectures.<sup>11,12</sup> More recently, our group reported a series of uranyl coordination polymers with green light emission by using flexible tricarboxylate and hexacarboxylate ligands.<sup>13</sup>

Encouraged by our previous studies, we chose 4,4'-oxidiphthalic acid as the bridging ligand to isolate uranyl complexes in this work. The considerations were as follows: (a) the V-shaped tetracarboxylate ligand exhibits flexibility around the center oxygen atom, and (b) four carboxylate functions can be completely or partially deprotonated, thus leading to varied coordination manners for binding uranium centers. Although previous studies demonstrate this tetracarboxylate ligand is a good candidate for the construction of transition metal

Received: July 25, 2014

Revised: September 28, 2014

Published: October 3, 2014

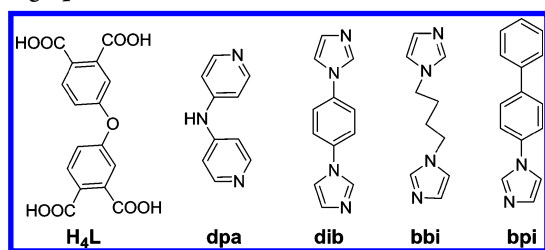
coordination polymers with diverse structures,<sup>14</sup> it is a seminal finding that this ligand serves as a building block for the construction of actinide polymeric structures. In this study, six uranyl compounds of 4,4'-oxidiphthalic acid in the presence of N-bearing species were synthesized, namely, (H<sub>2</sub>dpa)UO<sub>2</sub>L·3H<sub>2</sub>O (**1**), (H<sub>2</sub>dib)UO<sub>2</sub>L·H<sub>2</sub>O (**2**), (H<sub>2</sub>bbi)(UO<sub>2</sub>)L·3H<sub>2</sub>O (**3**), (H<sub>2</sub>dib)(dib)<sub>0.5</sub>[UO<sub>2</sub>L(dib)]·3H<sub>2</sub>O (**4**), (H<sub>2</sub>bbi)(U<sub>2</sub>O<sub>5</sub>)L·2H<sub>2</sub>O (**5**), and (Hbpi)<sub>2</sub>(UO<sub>2</sub>F)<sub>2</sub>L (**6**) [dpa = di(pyridin-4-yl)amine, dib = 1,4-di(1H-imidazol-1-yl)benzene, bbi = 1,1'-(1,4-butanediyl)bis(imidazole), bpi = 1-(biphenyl-4-yl)-1H-imidazole]. Their syntheses, structures, photoluminescence, and photocatalyses have been studied.

## EXPERIMENTAL SECTION

**Caution!** Standard procedures for handling radioactive material should be followed, although the uranyl compounds used in the lab contained depleted uranium.

**Materials, Syntheses, and Characterization.** All chemicals were purchased commercially and used without further purification. The carboxylate ligand and N-heterocyclic derivatives used in this work are shown in Scheme 1. Powder X-ray diffraction (PXRD) patterns were

**Scheme 1. Representation of the Carboxylate Ligand and N-Bearing Species**



performed on a D8 Focus (Bruker) diffractometer with Cu K $\alpha$  radiation field emission ( $\lambda = 1.5405$  Å, continuous, 40 kV, 40 mA, increment of 0.02°). Infrared spectra were collected from single crystals of all the uranyl compounds using a Nicolet 6700 Fourier transform infrared spectrometer with a diamond ATR objective. Energy dispersion X-ray (EDX) analysis was conducted with an FEI/

Philips XL30 ESEM-FEG instrument. The solid-state diffuse-reflectance UV–vis spectra for powder samples were recorded on a Shimadzu UV-3600 UV–vis spectrometer. The photoluminescence (PL) excitation and emission spectra were recorded with a model F-7000 luminescence spectrometer equipped with a 450 W xenon lamp as an excitation light source. The photomultiplier tube voltage was 400 V and the scan speed 1200 nm min<sup>−1</sup>, and the excitation and emission slit widths were both 5.0 nm. The photocatalytic system for the catalytic reaction included a 300 W Xe arc lamp (PLS-SXE300, Beijing Trustech Co.). The concentration of rhodamine B (RhB) was analyzed through a UV–vis spectrophotometer (Shimadzu, UV-3600) by checking the absorbance at 554 nm.

**Syntheses.** UO<sub>2</sub>(NO<sub>3</sub>)<sub>2</sub>·6H<sub>2</sub>O (50 mg, 0.1 mmol) or UO<sub>2</sub>(OAc)<sub>2</sub>·2H<sub>2</sub>O (40 mg, 0.1 mmol for **4** and **6**), 4,4'-oxidiphthalic acid (35 mg, 0.1 mmol), and deionized water (1.0 or 3.0 mL for **4** and **5**) were loaded into a 20 mL Teflon-lined stainless steel autoclave in the presence of dpa (17 mg, 0.1 mmol for **1**), dib (21 mg, 0.1 mmol for **2**, and 42 mg, 0.2 mmol for **4**), bbi (19 mg, 0.1 mmol for **3** and **5**), or bpi (22 mg, 0.1 mmol) and HF (40%, 25  $\mu$ L for **6**) to produce the title compounds. After being heated at 160 °C for 3 days, the autoclaves were then cooled to room temperature naturally. Yellow rod crystals of **1**, block crystals of **2**, **3**, and **5**, and tablets of **4** and **6** suitable for X-ray diffraction studies were obtained. Yields are 15% for **1**, 65% for **2**, 40% for **3**, 20% for **4**, 45% for **5**, and 60% for **6** based on uranium. Compound **4** is the minor phase combined with major unidentified powder. Phase purities except **4** were confirmed by powder X-ray diffraction patterns (Figures S1–S5 of the Supporting Information). The addition of HF is essential for the synthesis of compound **6**, in which HF acts as both a mineralizing agent and a bridging ligand. Compound **6** cannot be obtained without HF.

**Photocatalytic Test.** The typical photocatalytic degradation process is arranged as follows. An 80 mL aqueous solution of 10 mg L<sup>−1</sup> RhB was placed in a quartz beaker, and 50 mg of powder of the title compound was added then. Prior to irradiation, the suspension was sonicated for 5 min and then magnetically stirred in the dark for 30 min to reach the desorption–adsorption equilibrium. Afterward, the solution was under the irradiation of a 300 W Xe arc lamp. During irradiation, 3 mL of the suspension was continually taken from the reaction cell at ~30 min intervals. Suspensions were sampled and centrifuged with a TGL-16G centrifuge at 9000 rpm for 5 min to remove the uranyl sample and then analyzed by a UV–vis

**Table 1. Crystal Data and Structural Refinement for Title Compounds**

	1	2	3	4	5	6
empirical formula	C <sub>26</sub> H <sub>23</sub> N <sub>3</sub> O <sub>14</sub> U	C <sub>28</sub> H <sub>18</sub> N <sub>4</sub> O <sub>12</sub> U	C <sub>26</sub> H <sub>22</sub> N <sub>4</sub> O <sub>14</sub> U	C <sub>46</sub> H <sub>33</sub> N <sub>10</sub> O <sub>14</sub> U	C <sub>26</sub> H <sub>23</sub> N <sub>4</sub> O <sub>16</sub> U <sub>2</sub>	C <sub>46</sub> H <sub>32</sub> F <sub>2</sub> N <sub>4</sub> O <sub>13</sub> U <sub>2</sub>
Fw	839.5	840.49	852.51	1187.85	1122.54	1362.82
T (K)	296(2)	293(2)	293(2)	296(2)	293(2)	296(2)
crystal system	triclinic	monoclinic	triclinic	monoclinic	monoclinic	monoclinic
space group	$P\bar{1}$	$P2_1/n$	$P\bar{1}$	$P2_1/n$	$P2_1/n$	$C2/c$
a (Å)	8.991(2)	12.3655(9)	11.0082(7)	11.408(2)	15.8932(12)	30.514(2)
b (Å)	11.589(3)	16.4911(12)	11.9635(8)	32.504(6)	9.6528(7)	7.7560(6)
c (Å)	13.497(4)	14.7331(10)	12.6607(8)	12.620(3)	20.5316(16)	18.6624(15)
$\alpha$ (deg)	92.145(6)	90	87.1870(10)	90	90	90
$\beta$ (deg)	101.517(6)	114.511(2)	64.9680(10)	93.819(4)	99.859(2)	105.407(2)
$\gamma$ (deg)	97.816(6)	90	71.5000(10)	90	90	90
V (Å <sup>3</sup> )	1362.1(6)	2733.6(3)	1425.63(16)	4669.2(15)	3103.3(4)	4258.1(6)
Z, $\rho_{\text{calcd}}$ (Mg/m <sup>3</sup> )	2, 2.047	4, 2.042	2, 1.986	4, 1.609	4, 2.403	4, 2.126
$\mu$ (Mo K $\alpha$ ) (mm <sup>−1</sup> )	6.039	6.014	5.772	3.555	10.506	7.680
F(000)	808	1608	820	2332	2072	2568
R(int)	0.0370	0.0718	0.0318	0.0563	0.0742	0.0636
goodness of fit	1.027	0.969	1.046	1.018	0.972	1.004
$R_1/wR_2$ [ $I > 2\sigma(I)$ ] <sup>a</sup>	0.0370/0.0738	0.0417/0.0798	0.0413/0.0939	0.0453/0.1264	0.0408/0.0700	0.0387/0.0692
$R_1/wR_2$ (all data)	0.0448/0.0778	0.0694/0.0900	0.0518/0.0991	0.0694/0.1416	0.0812/0.0834	0.0566/0.0754

<sup>a</sup> $R_1 = \sum[\Delta F/\sum(F_0)]$ ;  $wR_2 = \{\sum[w(F_0^2 - F_c^2)]\}/\sum[w(F_0^2)^{1/2}]$ , where  $w = 1/\sigma^2(F_0^2)$ .

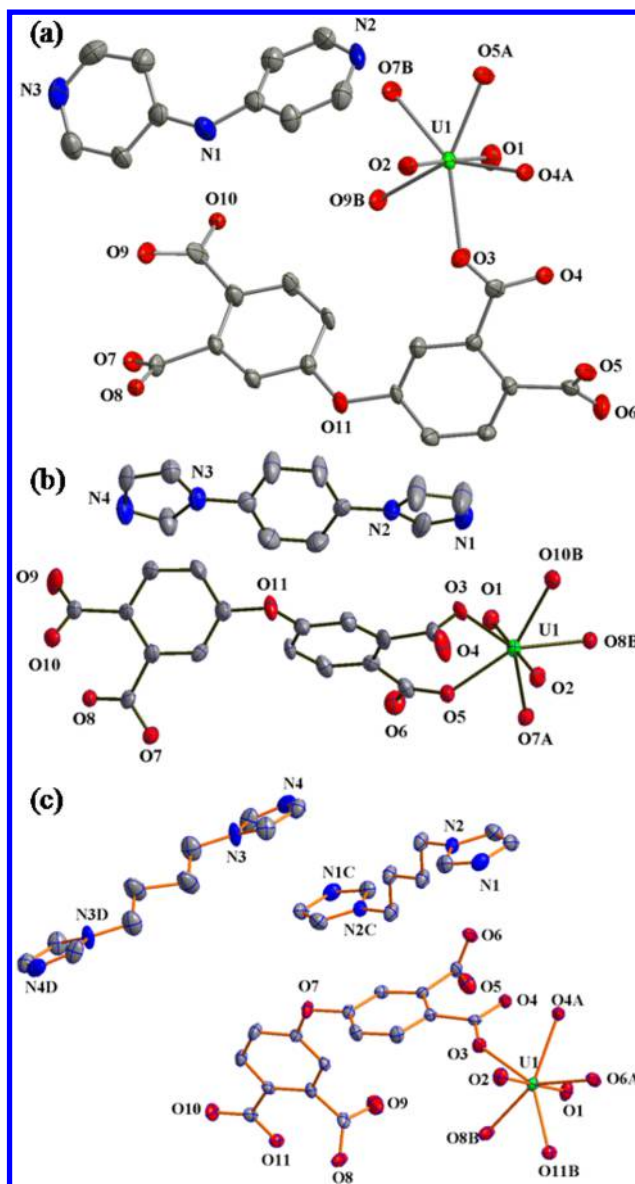
spectrophotometer. The characteristic absorption of RhB at  $\sim 554$  nm was chosen to supervise the photocatalytic degradation process.

**Determination of the X-ray Crystal Structure.** Single-crystal X-ray diffraction analyses were performed on selected suitable single crystals for title compounds. Crystallographic data were collected on a Bruker Apex II CCD diffractometer with graphite-monochromated Mo  $K\alpha$  radiation ( $\lambda = 0.71073$  Å). Data processing was accomplished with SAINT.<sup>15</sup> The crystal structures were determined by direct methods and refined on  $F^2$  by full-matrix least-squares using SHELXTL-97.<sup>16</sup> The final refinements included anisotropic displacement parameters for all non-hydrogen atoms. All hydrogen atoms were placed by geometrical considerations with isotropic displacement parameters equal to 1.2 times those of the parent atoms and were added to the structure factor calculation. A summary of the crystallographic data for these title compounds are listed in Table 1. Selected bond distances and angles are given in Tables S1–S6 of the Supporting Information.

## RESULTS AND DISCUSSION

**Structural Descriptions.** Compounds 1–3 contain similar skeleton structures, which incorporate common  $\text{UO}_7$  pentagonal bipyramids (Figure 1). These  $\text{UO}_7$  polyhedra are bridged by tridentate ligands, forming a one-dimensional ribbonlike structure (Figures 2–4). There is a unique uranium center in the asymmetric unit of each compound. This uranium atom is coordinated by two linear oxo atoms in the axis, and five equatorial oxygen atoms from three ligands, thereby creating a pentagonal bipyramid, which is the common coordination state of U(VI). The  $\text{U}=\text{O}$  bond lengths are 1.761(4) and 1.763(4) Å in 1, 1.761(5) and 1.770(5) Å in 2, and 1.757(5) and 1.763(5) Å in 3. The equatorial oxygen atoms are arranged from the uranium center at distances of 2.334(4)–2.398(4) Å in 1, 2.325(4)–2.403(4) Å in 2, and 2.327(5)–2.404(5) Å in 3. The calculated bond valence sum based on these values gives a uranium valence state of 6.24 in 1 and 3 and 6.15 in 2. These calculated values are consistent with the formal valence of U(VI).<sup>17</sup> The carboxylate ligand adopts tridentate model  $\mu_3(\eta_2:\eta_2:\eta_1)$  by linking three uranyl centers in these one-dimensional structures (Scheme 2). As the flexibility of the ligand, it exhibits different configurations in these assemblies. It is more bent in 3; thus, the length of the periodic unit in 3 (12.8 Å) is shorter than that in 1 and 2 (14.6 and 14.7 Å, respectively). Such ribbon structures are anionic; to keep the charge balance, protonated dpa, dib, and bbi exist in compounds 1–3, respectively. The N-bearing templating molecules interact with the one-dimensional structures via hydrogen bonds ( $\text{N}-\text{H}\cdots\text{O}$ , 2.61–2.98 Å). In compound 2, weak  $\pi-\pi$  interaction exists between neighboring dib molecules with an intercentroid distance of 3.98 Å. For compound 3, the skeleton and the bbi molecules also interact through  $\pi-\pi$  stacking with intercentroid distances of 3.63–3.81 Å.

Compound 4 crystallizes in monoclinic space group  $P2_1/n$ . The asymmetric unit consists of one uranium atom, one L ligand, and two and one-half dib molecules. As shown in Figure 5a, the U atom is seven-coordinated by two axial oxo atoms, four equatorial O atoms from two L ligands, and one N atom from one dib molecule, forming a common pentagonal bipyramid. The  $\text{U}=\text{O}$  distances in the axis are 1.746(6) and 1.778(6) Å. The  $\text{U}-\text{O}$  bond lengths in the equatorial plane are in the range of 2.324(5)–2.382(5) Å, while the  $\text{U}-\text{N}$  connection is longer with a bond length of 2.540(6) Å. The calculated bond valence sum indicates 6.05 for U(1). The bridging L ligand links the nearby two U centers in a  $\mu_2(\eta_2:\eta_2)$  manner, forming an assembly of one-dimensional chains





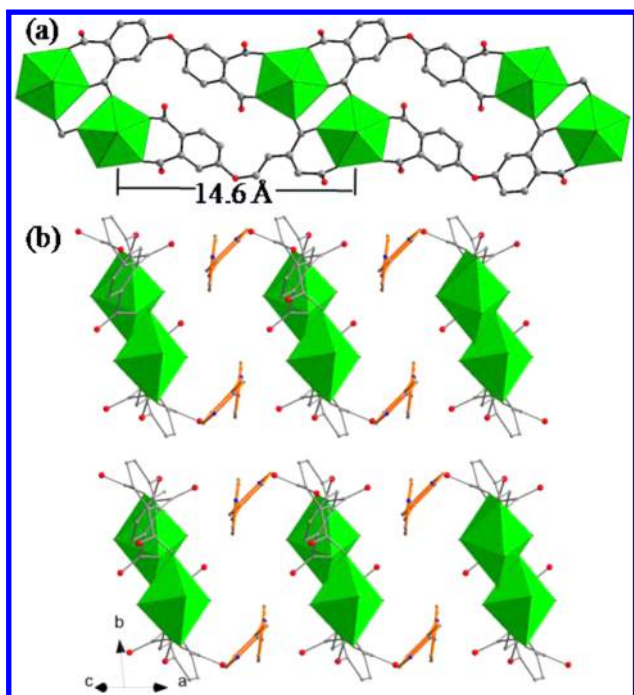


**Figure 2.** (a) One-dimensional structure in 1. (b) View of the whole structure showing the packing of such ribbons and dpa templates.

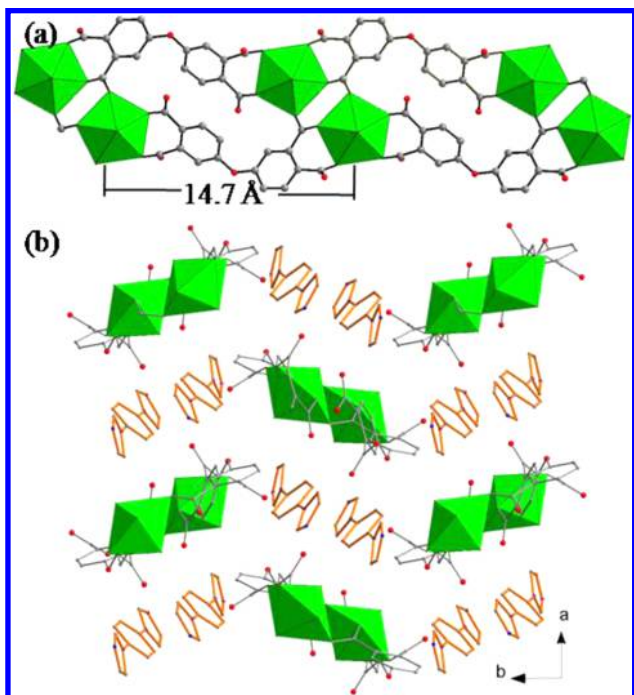


**Figure 3.** (a) One-dimensional ribbon structure isolated from 2. (b) View along the [001] direction showing the packing mode of such assemblies.

oxygen surrounding, in which the equatorial plane is formed by one bridging  $\mu_3$ -O atom and four oxygen atoms from two L ligands. The oxygen surrounding of U(2) is a hexagonal bipyramid, which incorporates two bridging  $\mu_3$ -O atoms and four oxygen atoms from two L ligands. The average U=O bond lengths along the axis are 1.7651(5) Å for U(1) and 1.759(6) Å for U(2). The U–O bond distances in the equatorial plane are in the range of 2.189(6)–2.449(7) Å for

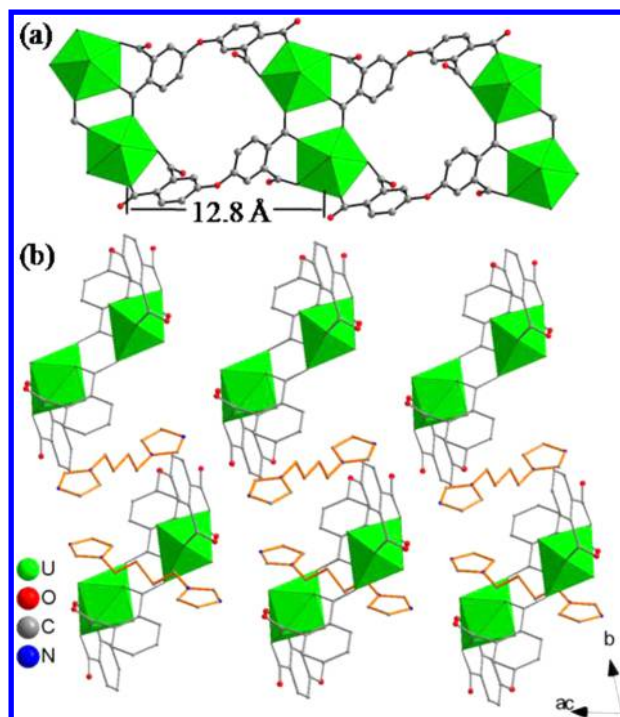
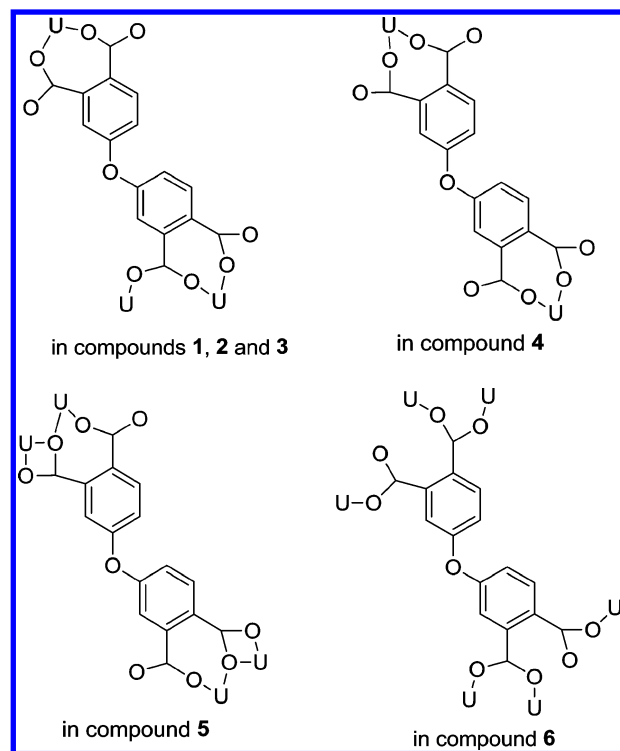


**Figure 4.** (a) Ribbon assembly in 3. (b) View of the whole structure showing the location of the uranyl carboxylate skeleton and bbi templates.

#### Scheme 2. Summary of Coordination Modes of 4,4'-Oxydiphthalic Acid in Synthesized Uranyl Compounds



U(1) and 2.236(6)–2.668(6) Å for U(2). The longer distances are reasonable for an eight-coordinated U(VI) center.<sup>17a</sup> Bond valence sum indicates 6.28 for U(1) and 6.26 for U(2), which is in agreement with the formal state of U(VI). Each bridging  $\mu_3$ -O(1) atom combines one  $\text{UO}_7$  pentagonal and two  $\text{UO}_8$

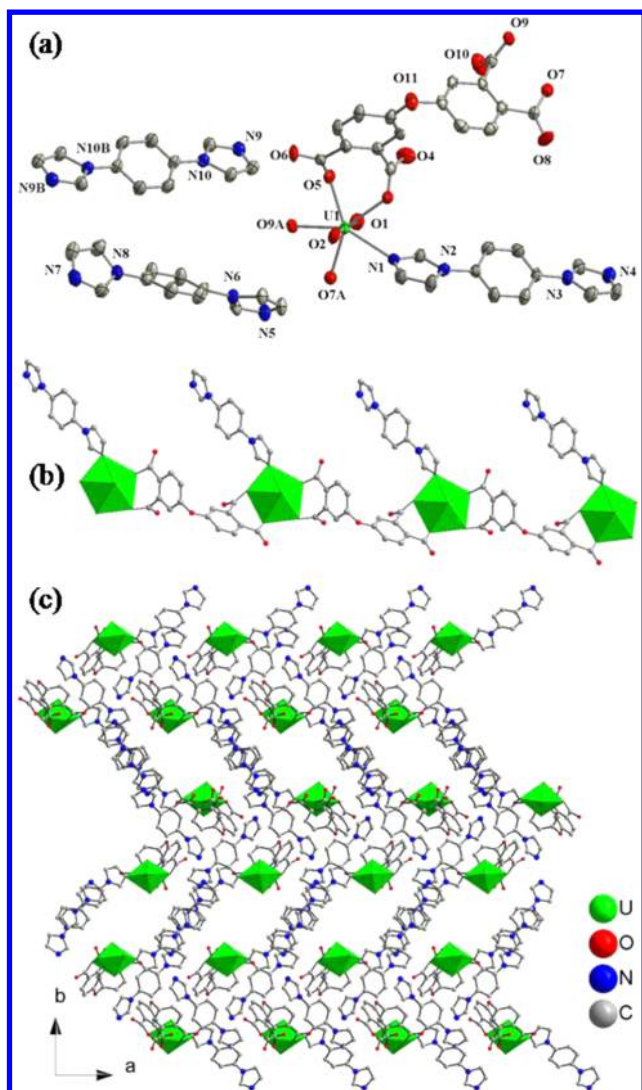


**Figure 5.** (a) Coordination environment in **4**. Displacement ellipsoids are drawn at the 50% probability level. Symmetry codes: A,  $x, y, 1 + z$ ; B,  $1 - x, 2 - y, 1 - z$ . (b) One-dimensional chain structure of **4** formed by  $\text{UO}_7$  pentagonal bipyramids, carboxylate, and dib ligands. (c) View of the packing of such chains along the  $c$  axis.

hexagonal bipyramids, and two  $\mu_3$ -O atoms form a common edge of two hexagonal bipyramids, which further share edges with peripheral pentagonal bipyramids. Then a centrosymmetrical tetramer is combined. Such tetranuclear motifs, which serve as the secondary building units, are linked by tetradentate L ligands forming a two-dimensional network of this compound (Figure 6b). The layered assemblies are packed to make the three-dimensional supramolecular structure via  $\pi$ - $\pi$  interaction with an intercentroid distance of 3.64 Å (Figure 6c). Protonated bbi molecules are accommodated in the void space of this frame.

In this structure, the carboxylate ligand as a  $\mu_4$  ( $\eta_2:\eta_2:\eta_2:\eta_2$ ) bridging linker connects four uranyl centers from two tetranuclear motifs. Notably, the tetranuclear motif has been involved in only six uranyl carboxylates, in which three isostructures are zero-dimensional clusters templated by different counterions.<sup>18</sup> Two isotype representatives incorporate the tetranuclear motifs and a uranyl dimer, forming one-dimensional ribbon arrangements.<sup>19</sup> The last example represents a one-dimensional infinite-chain assembly formed by

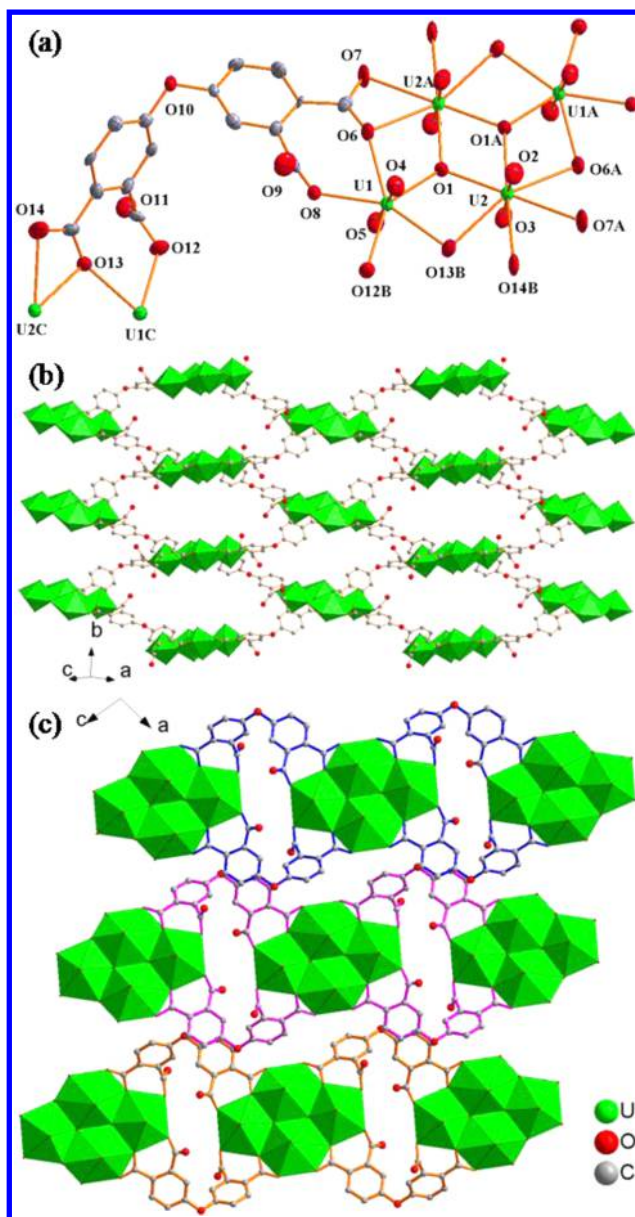


**Figure 6.** (a) Coordination environment in **5**. Displacement ellipsoids are drawn at the 50% probability level. Symmetry codes: A,  $1 - x, 1 - y, -z$ ; B,  $0.5 - x, 0.5 + y, 0.5 - z$ ; C,  $0.5 - x, -0.5 + y, 0.5 - z$ . (b) Layered structure of **5** formed by tetranuclear building units and ligands. (c) View of the packing of such layers along the  $b$  axis. bbi has been omitted for the sake of clarity.

corner-sharing mononuclear  $\text{UO}_8$  and this tetranuclear entity.<sup>20</sup> As far as we know, compound **5** is the first extended network structure of uranyl carboxylate featuring such a tetranuclear secondary building unit.

Compound **6** is the only F-bearing uranyl coordination polymer in this work (Figure 7a). It consists of uranyl cations in the form of  $\text{UO}_5\text{F}_2$  pentagonal bipyramids, which are condensed via corner sharing into a chain structure. The chains are linked by tetradentate carboxylate ligands into a layered structure (Figure 7b). In this sheet, the uranium is bound to two axial oxygen atoms with  $\text{U}=\text{O}$  distances of 1.757(4) and 1.763(4) Å. Three  $\text{U}-\text{O}$  bonds along the equatorial axis are in the distance range of 2.343(5)–2.419(4) Å, which are longer than  $\text{U}-\text{F}$  bond lengths of 2.295(3) and 2.305(3) Å. The assignment of the F atom is according to the



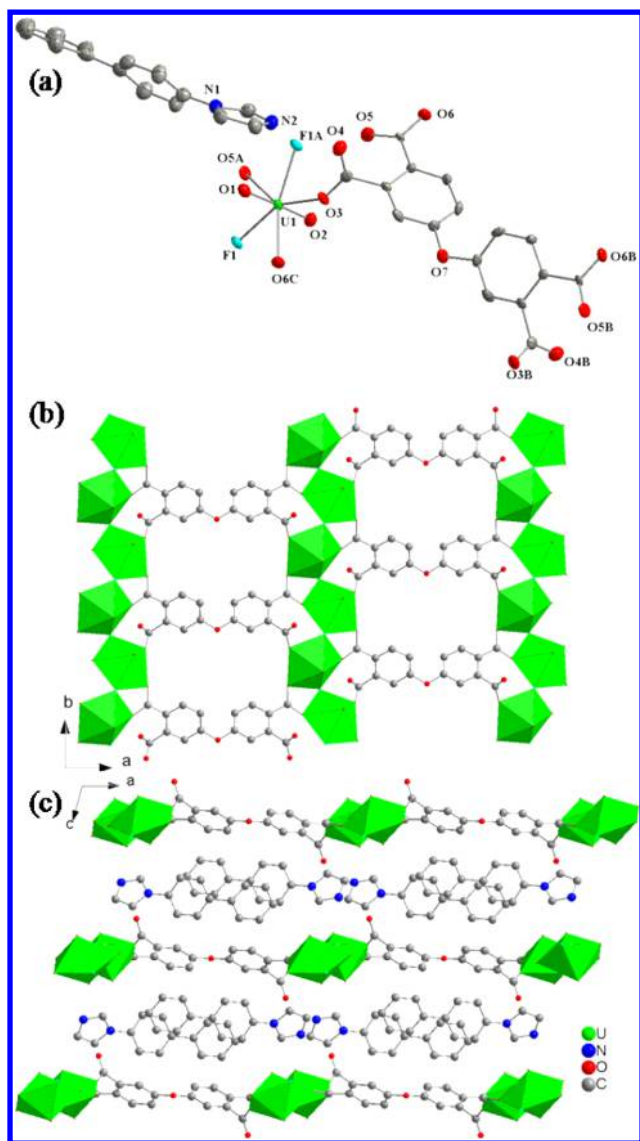


**Figure 7.** (a) Coordination environment in **6**. Displacement ellipsoids are drawn at the 50% probability level. Symmetry codes: A,  $0.5 - x, -0.5 + y, 1.5 - z$ ; B,  $1 - x, y, 1.5 - z$ ; C,  $x, 1 + y, z$ . (b) Layered structure of **6** formed by corner-sharing uranyl chains and ligands. (c) bpi molecules are located between such layers.

improvement of the refinement when the F atom was selected instead of the O atom. Further confirmation was supplied by energy dispersive X-ray spectroscopy (Figure S6 of the Supporting Information). Bond valence sum gives 6.05 for the U atom and 0.83 and 0.86 for the two coordinating F atoms based on these U–O and U–F bond values. The ligand serves as a  $\mu_4$  ( $\eta_1:\eta_1:\eta_1:\eta_1$ ) bridging linker by connecting four uranium centers. Protonated bpi molecules are between the layers and compensate for the anionic charge of the layered structure (Figure 7c).

**Infrared (IR) Spectroscopy.** IR spectra of these synthesized uranyl carboxylates are displayed in Figure S7 of the Supporting Information. The stretching vibrations of OH groups are indicated around  $3600\text{ cm}^{-1}$ . The peaks in the range of  $3130\text{--}3000\text{ cm}^{-1}$  are attributed to the C–H stretching modes of the aromatic rings. The absorption bands in the ranges of  $1320\text{--}1480$  and  $1600\text{--}1650\text{ cm}^{-1}$  are due to  $\nu_{\text{sym}}(\text{COO})$  and  $\nu_{\text{asym}}(\text{COO})$  stretching modes, respectively.

The bending vibrations of C–H groups in the aromatic rings range from  $1160$  to  $650\text{ cm}^{-1}$ . The peaks around  $930$  and  $830\text{ cm}^{-1}$  may be due to symmetrical  $\nu_1$  and antisymmetric elongations  $\nu_3$  of  $\text{UO}_2^{2+}$  cations, respectively.

**Luminescence Property.** The charge-transfer-based emission of green light from uranyl-bearing compounds has been documented for decades. This emission always comprises several peaks in the spectrum, which is vibronically coupled to the symmetric and antisymmetric vibrational modes of the uranyl cation.<sup>21</sup> The excitation and emission spectra of these uranyl compounds were studied (Figures S8–S12 of the Supporting Information and Figure 8). As depicted in Figure 8,

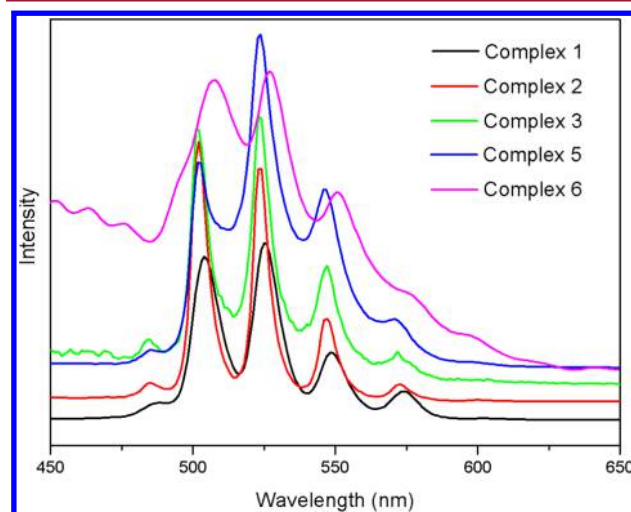


**Figure 8.** Emission spectra of **1** ( $\lambda_{\text{ex}} = 283\text{ nm}$ ), **2** ( $\lambda_{\text{ex}} = 275\text{ nm}$ ), **3** ( $\lambda_{\text{ex}} = 270\text{ nm}$ ), **5** ( $\lambda_{\text{ex}} = 277\text{ nm}$ ), and **6** ( $\lambda_{\text{ex}} = 217\text{ nm}$ ) showing the green light emission from uranyl dications.

four well-resolved sharp vibronic peaks centered at 502, 523, 546, and 572 nm are clearly demonstrated by compounds **2**, **3**, and **5**. They differ only in resolution. For compound **1**, well-defined charge-transfer vibronic transitions are also represented by four emission peaks with a slight red shift of 2 nm compared to compound **2**. For compound **6**, three prominent peaks are observed at 508, 527, and 551 nm in its spectrum. These emission peaks correspond to the electronic and vibronic transitions  $S_{11}\text{--}S_{00}$  and  $S_{10}\text{--}S_{0v}$  ( $v = 0\text{--}4$ ).<sup>22</sup> Compared with the benchmark compound  $\text{UO}_2(\text{NO}_3)_2 \cdot 6\text{H}_2\text{O}$ , compound **6** exhibits the greatest red shift of 18 nm followed by compounds **1** (16 nm) and **2**, **3**, and **5** (14 nm). The difference may be due to the coordination surrounding of uranium,  $\text{UO}_7$ ,  $\text{UO}_8$ ,  $\text{UO}_6\text{N}$ , and  $\text{UO}_5\text{F}_2$  polyhedral environments, and the influence of coordinated carboxylate and imidazole ligands as well as N-donor templates.

**Photocatalysis Test.** The photocatalytic performance of uranyl ions has been investigated since the 1800s, and the attractive photocatalytic activity is ascribed to the presence of the intrinsic  $\text{U}=\text{O}$  bond.<sup>23</sup> Recently, Chen et al. studied the heterogeneous photocatalysis of RhB by using uranyl inorganic–organic hybrid compounds and proposed the photodegradation (oxidation) mechanism of RhB in the presence of uranyl compounds.<sup>7a–c</sup> As revealed by UV–vis spectroscopy of these synthesized uranyl compounds (Figure S13 of the Supporting Information), the absorptions in the region of  $380\text{--}500\text{ nm}$  (centered at  $\sim 430\text{ nm}$ ) are observed, which are ascribed to the charge-transfer transitions within the

uranyl group. The presence of vis adsorption motivates us to investigate the heterogeneous photocatalytic properties of these uranyl coordination polymers under visible light. To study the photocatalytic properties, RhB, an organic pollutant that is difficult to degrade, was selected as the model of dye contaminant under visible light illumination. Control experiments were conducted on an RhB solution in the absence of these uranyl samples. Almost no degradation of the dye was displayed in the absence of a catalyst when the irradiation time of RhB was increased to 3 h (Figure S14 of the Supporting Information). In contrast, in the presence of synthesized uranyl compounds, the intensities of the characterized absorption peaks of RhB decrease rapidly followed by a gradual hypsochromic shift (Figures S15–S18 of the Supporting Information). As shown in Figure 9, when RhB was illuminated

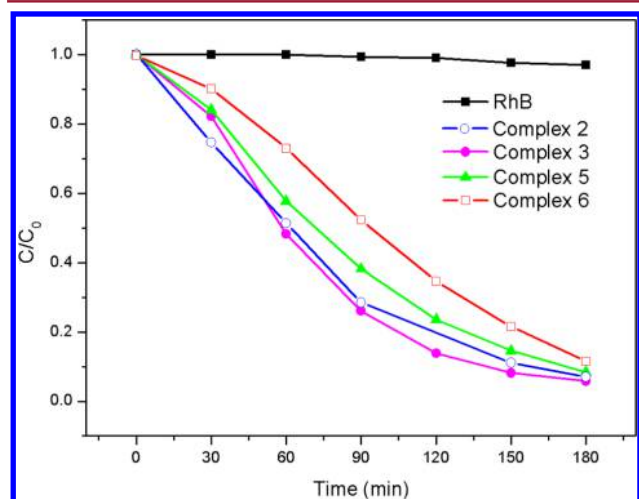


**Figure 9.** Changes in the concentration of RhB irradiated with Xe light as a function of irradiation time in the presence of synthesized uranyl compounds and the control experiment without any catalyst under the same conditions.  $C$  and  $C_0$  stand for the RhB concentrations after and before irradiation, respectively.

for 3 h, the targeted dye degraded ~93.0% for 2, ~94.2% for 3, ~91.6% for 5, and ~88.3% for 6. These results clearly indicate that these uranyl coordination polymers have important effects on the photodecomposition of RhB. The mechanism involving photoexcitation of uranyl centers and molecular oxygen probably accounts for the photocatalysis of RhB. The blue shift of adsorption peaks can be attributed to N-deethylation of RhB after photocatalysis; concurrently, the chromophore of RhB is broken down as the dye is degraded.<sup>24</sup> The photocatalytic performance of 1 and 4 was not evaluated because of low yield or impurity.

## CONCLUSION

In summary, a series of uranyl coordination polymers based on 4,4'-oxidiphthalic acid have been synthesized. These compounds feature one-dimensional chain or ribbon structures and two-dimensional layered architectures, in which uranium centers exist in the form of common pentagonal bipyramids, tetranuclear motifs, or chains of edge-sharing of  $\text{UO}_2\text{F}_2$  pentagonal bipyramids. The N-bearing species serve as templates, counterions, and coligands. Typical green light emissions of  $\text{UO}_2^{2+}$  cations are represented, and rhodamine B molecules could be decomposed efficiently under visible light irradiation by these compounds. Future work is necessary to

investigate the effect on structures and photochemical properties by adding transition metal atoms.

## ASSOCIATED CONTENT

### Supporting Information

X-ray crystallographic cif files, selected bond lengths and angles, powder X-ray diffraction patterns, EDX spectroscopy, IR spectra, excitation spectra, UV–vis diffuse-reflectance spectra, and absorption spectra of the RhB solution with and without a catalyst. This material is available free of charge via the Internet at <http://pubs.acs.org>.

## AUTHOR INFORMATION

### Corresponding Author

\*E-mail: [szm@ciac.ac.cn](mailto:szm@ciac.ac.cn).

### Author Contributions

W.Y. and W.-G.T. contributed equally to this work.

### Notes

The authors declare no competing financial interest.

## ACKNOWLEDGMENTS

We are grateful for the support of this work by the National Nature Science Foundation of China (21171162, 21301168, and 21401188), the Jilin Province Youth Foundation (20130522132JH and 20130522123JH), and SRF for ROCS (State Education Ministry).

## REFERENCES

- (1) (a) Wang, Z.; Cohen, S. M. *Chem. Soc. Rev.* **2009**, *38*, 1315. (b) Bloch, E. D.; Queen, W. L.; Krishna, R.; Zadrozny, J. M.; Brown, C. M.; Long, J. R. *Science* **2012**, *335*, 1606. (c) Horike, S.; Shimomura, S.; Kitagawa, S. *Nat. Chem.* **2009**, *1*, 695. (d) Kreno, L. E.; Leong, K.; Farha, O. K.; Allendorf, M.; Van Duyne, R. P.; Hupp, J. T. *Chem. Rev.* **2012**, *112*, 1105.
- (2) (a) Wang, X.-S.; Ma, S.; Sun, D.; Parkin, S.; Zhou, H.-C. *J. Am. Chem. Soc.* **2006**, *128*, 16474. (b) Hawxwell, S. M.; Espallargas, G. M.; Bradshaw, D.; Rosseinsky, M. J.; Prior, T. J.; Florence, A. J.; Van de Streek, J.; Brammer, L. *Chem. Commun.* **2007**, 1532. (c) Wang, X.-L.; Qin, C.; Wang, E.-B.; Li, Y.-G.; Su, Z.-M.; Xu, L.; Carlucci, L. *Angew. Chem., Int. Ed.* **2005**, *44*, 5824. (d) Yi, F. Y.; Zhang, J.; Zhang, H. X.; Sun, Z. M. *Chem. Commun.* **2012**, 48, 10419.
- (3) (a) Wang, S. A.; Villa, E. M.; Diwu, J. A.; Alekseev, E. V.; Depmeier, W.; Albrecht-Schmitt, T. E. *Inorg. Chem.* **2011**, *50*, 2527. (b) Wang, S. A.; Alekseev, E. V.; Stritzinger, J. T.; Liu, G. K.; Depmeier, W.; Albrecht-Schmitt, T. E. *Chem. Mater.* **2010**, *22*, 5983. (c) Wang, S. A.; Alekseev, E. V.; Stritzinger, J. T.; Depmeier, W.; Albrecht-Schmitt, T. E. *Inorg. Chem.* **2010**, *49*, 2948. (d) Diwu, J.; Wang, S.; Albrecht-Schmitt, T. E. *Inorg. Chem.* **2012**, *51*, 4088.
- (4) (a) Wang, C. M.; Lii, K. H. *J. Solid State Chem.* **2013**, *197*, 456. (b) Chen, C. S.; Kao, H. M.; Lii, K. H. *Inorg. Chem.* **2005**, *44*, 935. (c) Nguyen, Q. B.; Chen, C. L.; Chiang, Y. W.; Lii, K. H. *Inorg. Chem.* **2012**, *51*, 3879. (d) Chen, C. L.; Nguyen, Q. B.; Chen, C. S.; Lii, K. H. *Inorg. Chem.* **2012**, *51*, 7463. (e) Lin, C.-H.; Lii, K.-H. *Angew. Chem., Int. Ed.* **2008**, *47*, 8711.
- (5) (a) Ling, J.; Qiu, J.; Szymanowski, J. E. S.; Burns, P. C. *Chem.—Eur. J.* **2011**, *17*, 2571. (b) Qiu, J.; Burns, P. C. *Chem. Rev.* **2013**, *113*, 1097. (c) Cantos, P. M.; Jouffret, L. J.; Wilson, R. E.; Burns, P. C.; Cahill, C. L. *Inorg. Chem.* **2013**, *52*, 9487.
- (6) (a) Wang, K. X.; Chen, J. S. *Acc. Chem. Res.* **2011**, *44*, 531. (b) Yu, Z. T.; Liao, Z. L.; Jiang, Y. S.; Li, G. H.; Chen, J. S. *Chem.—Eur. J.* **2005**, *11*, 2642. (c) Liao, Z. L.; Li, G. D.; Bi, M. H.; Chen, J. S. *Inorg. Chem.* **2008**, *47*, 4844. (d) Chen, W.; Yuan, H. M.; Wang, J. Y.; Liu, Z. Y.; Xu, J. J.; Yang, M.; Chen, J. S. *J. Am. Chem. Soc.* **2003**, *125*, 9266. (e) Yu, Z. T.; Liao, Z. L.; Jiang, Y. S.; Li, G. H.; Li, G. D.; Chen, J. S. *Chem. Commun.* **2004**, 1814.



- (7) (a) Loiseau, T.; Mihalcea, I.; Henry, N.; Volklinger, C. *Coord. Chem. Rev.* **2014**, 266–267, 69. (b) Olchowka, J.; Falaise, C.; Volklinger, C.; Henry, N.; Loiseau, T. *Chem.—Eur. J.* **2013**, 19, 2012. (c) Volklinger, C.; Henry, N.; Grandjean, S.; Loiseau, T. *J. Am. Chem. Soc.* **2012**, 134, 1275. (d) Mihalcea, I.; Volklinger, C.; Henry, N.; Loiseau, T. *Inorg. Chem.* **2012**, 51, 9610.
- (8) (a) Adelani, P. O.; Albrecht-Schmitt, T. E. *Angew. Chem., Int. Ed.* **2010**, 49, 8909. (b) Adelani, P. O.; Albrecht-Schmitt, T. E. *Inorg. Chem.* **2011**, 50, 12184.
- (9) (a) Grohol, D.; Subramanian, M. A.; Poojary, D. M.; Clearfield, A. *Inorg. Chem.* **1996**, 35, 5264. (b) Gagnon, K. J.; Perry, H. P.; Clearfield, A. *Chem. Rev.* **2012**, 112, 1034.
- (10) (a) Yang, W. T.; Wu, H. Y.; Wang, R. X.; Pan, Q. J.; Sun, Z. M.; Zhang, H. J. *Inorg. Chem.* **2012**, 51, 11458. (b) Yang, W. T.; Tian, T.; Wu, H. Y.; Pan, Q. J.; Dang, S.; Sun, Z. M. *Inorg. Chem.* **2013**, 52, 2736. (c) Tian, T.; Yang, W. T.; Pan, Q. J.; Sun, Z. M. *Inorg. Chem.* **2012**, 51, 11150. (d) Yang, W.; Yi, F. Y.; Tian, T.; Tian, W. G.; Sun, Z. M. *Cryst. Growth Des.* **2014**, 14, 1366.
- (11) (a) Thuéry, P. *Cryst. Growth Des.* **2008**, 8, 4132. (b) Thuéry, P. *Cryst. Growth Des.* **2011**, 11, 2606. (c) Thuéry, P. *Cryst. Growth Des.* **2009**, 9, 4592. (d) Thuéry, P. *Cryst. Growth Des.* **2011**, 11, 347.
- (12) (a) Borkowski, L. A.; Cahill, C. L. *Cryst. Growth Des.* **2006**, 6, 2248. (b) Borkowski, L. A.; Cahill, C. L. *Inorg. Chem.* **2003**, 42, 7041. (c) Knope, K. E.; Cahill, C. L. *Inorg. Chem.* **2008**, 47, 7660.
- (13) (a) Wu, H. Y.; Wang, R. X.; Yang, W. T.; Chen, J. L.; Sun, Z. M.; Li, J.; Zhang, H. J. *Inorg. Chem.* **2012**, 51, 3103–3107. (b) Yang, W. T.; Dang, S.; Wang, H.; Tian, T.; Pan, Q. J.; Sun, Z. M. *Inorg. Chem.* **2013**, 52, 12394.
- (14) (a) Chu, Q.; Jian, Z. S.; Okamura, F. T.; Lv, G.-C.; Liu, G.-X.; Sun, W. Y.; Ueyama, N. *Cryst. Growth Des.* **2011**, 11, 3885. (b) Yang, J.-X.; Zhang, X.; Cheng, J.-K.; Zhang, J.; Yao, Y.-G. *Cryst. Growth Des.* **2012**, 12, 333. (c) Li, S.-L.; Lan, Y.-Q.; Ma, J.-C.; Ma, J.-F.; Su, Z.-M. *Cryst. Growth Des.* **2010**, 10, 1161. (d) Gong, Y.; Li, J.; Qin, J. B.; Lin, J. H. *CrystEngComm* **2012**, 14, 5862. (e) Li, S.-L.; Lan, Y.-Q.; Ma, J.-F.; Fu, Y.-M.; Yang, J.; Ping, G.-J.; Liu, J.; Su, Z.-M. *Cryst. Growth Des.* **2008**, 8, 1610. (f) Wang, H.; Yang, W. T.; Sun, Z. M. *Chem.—Asian J.* **2013**, 8, 982.
- (15) SMART and SAINT; Siemens Analytical X-ray Instruments, Inc.: Madison, WI, 1996.
- (16) SHELXTL, version 5.1; Siemens Industrial Automation, Inc.: Madison, WI, 1997.
- (17) (a) Burns, P. C.; Ewing, R. C.; Hawthorne, F. C. *Can. Min.* **1997**, 35, 1551. (b) Brese, N. E.; O'Keeffe, M. *Acta Crystallogr.* **1991**, B47, 192.
- (18) Charushnikova, I. A.; Krot, N. N.; Polyakova, I. N.; Makarenkov, V. I. *Radiochemistry* **2005**, 47, 241.
- (19) Mihalcea, I.; Henry, N.; Loiseau, T. *Cryst. Growth Des.* **2011**, 11, 1940.
- (20) Grigoriev, M. S.; Antipin, M. Y.; Krot, N. N. *Radiochemistry* **2004**, 46, 206.
- (21) Denning, R. G.; Norris, J. O. W.; Short, I. G.; Snellgrove, T. R.; Woodwark, D. R. *Lanthanide and Actinide Chemistry and Spectroscopy*; Edelstein, N. M., Ed.; ACS Symposium Series No. 131; American Chemical Society: Washington, DC, 1980; Chapter 15.
- (22) (a) Nelson, A. G. D.; Alekseev, E. V.; Ewing, R. C.; Albrecht-Schmitt, T. E. *J. Solid State Chem.* **2012**, 192, 153. (b) Jiang, Y. S.; Yu, Z. T.; Liao, Z. L.; Li, G. H.; Chen, J. S. *Polyhedron* **2006**, 25, 1359.
- (23) Burrows, H. D.; Kemp, T. J. *Chem. Soc. Rev.* **1974**, 139.
- (24) (a) Horikoshi, S.; Saitou, A.; Hidaka, H.; Serpone, N. *Environ. Sci. Technol.* **2003**, 37, 5813. (b) Takizawa, T.; Watanabe, T.; Honda, K. *J. Phys. Chem.* **1978**, 82, 1391. (c) Watanabe, T.; Takizawa, T.; Honda, K. *J. Phys. Chem.* **1977**, 81, 1845. (d) Wu, T.; Liu, G.; Zhao, J.; Hidaka, H.; Serpone, N. *J. Phys. Chem. B* **1999**, 103, 4862.